

# MONTE CARLO SIMULATION STUDY ON THE $^{241}\text{Am}$ -Be RADIONUCLIDE SOURCE REFERENCE NEUTRON RADIATION

by

**Yixin LIU**<sup>1,2</sup>, **Song ZHANG**<sup>1,3</sup>, **Yikun QIAN**<sup>1,3</sup>, **Yuchen HUANG**<sup>1,3</sup>,  
**Benjiang MAO**<sup>1</sup>, **Peng FENG**<sup>3</sup>, and **Zhiqiang CHEN**<sup>2\*</sup>

<sup>1</sup> Institute of Nuclear Physics and Chemistry, China Academy of Engineering Physics, Mianyang, China

<sup>2</sup> Department of Engineering Physics, Tsinghua University, Beijing, China

<sup>3</sup> Key Laboratory of Optoelectronics Technology and System, Ministry of Education, Chongqing University, Chongqing, China

Scientific paper

<https://doi.org/10.2298/NTRP2004283L>

In order to study the feasibility of using lightweight  $^{241}\text{Am}$ -Be radionuclide reference neutron radiation field for the calibration of neutron measurement instruments, this paper reported the Monte Carlo simulation work on free field reference neutron radiation, standard reference neutron radiation regulated by ISO-8529 series standards and minitype reference neutron radiation we designed. The distributions of dose equivalent rates and neutron energy spectrum in different conditions, such as different room types, different room sizes and different shield materials were the main simulation contents for analyzing the characteristics of the three types of reference neutron radiation. According to the simulation results, theoretical supports were provided for the discussion on the minitype reference neutron radiation for calibration purpose.

*Key words:* Monte Carlo,  $^{241}\text{Am}$ -Be radionuclide source, reference neutron radiation, neutron energy spectrum, dose equivalent rate

## INTRODUCTION

Neutron radiation metrology is important in radiation protection field [1]. Instruments applied for neutron radiation measurement, such as neutron ambient dose equivalent instrument, rem meter or neutron energy spectroscopy, are extremely important tools to ensure the safety of nuclear facilities and devices, as well as radioactive workers [2]. Termly calibrations should be taken out to ensure the performances of these instruments. Gressier *et al.* [3] explained the definition and technology status of calibration for neutron measurement instruments. At present, all calibration works of neutron measuring instruments should be carried out in reference to neutron radiations around the world. Radionuclide neutron sources, that are the reference standards because of the quantities, neutron fluence and neutron dose equivalent, can be realized in laboratories. So, they are of fundamental importance to neutron metrology [4]. The ISO-8529 series standards regulated the radionuclide sources applied for calibration purpose include  $^{241}\text{Am}$ -Be,  $^{252}\text{Cf}$ , and  $^{252}\text{Cf} + \text{D}_2\text{O}$  [5-7]. However, in most radiation protection situations, the neutron energy spectra are different

from those generated by radionuclide sources described above. Therefore, ISO-12789 series standards regulated the simulated workplace reference neutron radiation field, whose characteristics are more similar to the real measurements [8-10]. But, the simulated workplace reference neutron radiation is quite complex. The irradiation facility includes radionuclide source, accelerator, or reactor. Moreover, in order to achieve ideal neutron energy spectra, various absorbing, or scattered materials are placed between the primary neutron source and point of test, in order to change the distribution of neutron energy spectrum. Therefore, there are few metrological services equipped with simulated workplace reference neutron radiation. Last year the China Institute of Atomic Energy has built a simulated workplace reference neutron radiation and it was the first one in China. So, the general reference neutron radiation for calibration purpose is still generated by radionuclide sources, at present [11-13].

In the standard reference neutron radiation (SRNR) regulated by ISO-8529 series standards, contribution of scattered neutrons to the indication should be less than 40 %. This regulation not only eliminates the influence of scattered neutrons on the instrument indication from dosimetry view, but also prevents the

\* Corresponding author; e-mail: [c\\_thu1328@126.com](mailto:c_thu1328@126.com)

calibration deviation caused by the scattered neutrons with complex energy distribution, to the instruments with different energy responses. To meet the demands, the minimum size of the reference neutron radiation should not be less than  $3\text{ m} \times 3\text{ m} \times 3\text{ m}$  (open ceiling type room is smaller but the incompletely enclosed structure was not in consideration in this study) [5]. With the corresponding shield facilities, the heavy weight and large size make it inconvenient to move.

With the development of nuclear science and technology, the demands of in situ calibration of nuclear detectors are obviously increasing. In gamma metrology field, removable calibration devices are developed for the calibration of area and portable gamma detectors, as well as personal dosimeters [14, 15]. In neutron metrology field, no relative researches on such removable calibration devices are reported. Based on this, this work carried out a study on the Monte Carlo simulation on  $^{241}\text{Am}$ -Be reference neutron radiation. First, we simulated the free field reference neutron radiation (FRNR) and SRNR regulated by ISO-8529 series standards. Then we simulated a proposed minitype reference neutron radiation (MRNR) compared to the SRNR and discussed the feasibility of the MRNR application for calibrations of neutron measuring instruments.

## METHOD

The  $^{241}\text{Am}$ -Be reference neutron radiation model in this study included FRNR, SRNR regulated by ISO-8529 series standards and MRNR we designed. The energy distribution data of  $^{241}\text{Am}$ -Be source was from ISO-8529 and the spectrum were shown in fig. 1. The neutron emission rate was set as  $2.5 \cdot 10^6\text{ s}^{-1}$ . The Monte Carlo code Geant 4 was employed as simulation tool to calculate the mode [16-18].

In the description of the three types of reference radiation, some quantities would be mentioned repeatedly. Therefore, we will define them in advance.

- The distance between the point of test and  $^{241}\text{Am}$ -Be source was defined as  $D$ .

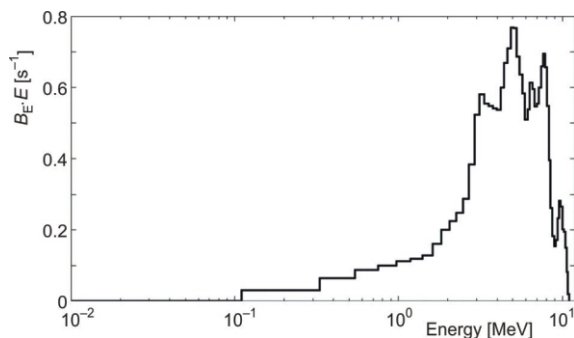


**Figure 1. Neutron energy spectrum of a  $^{241}\text{Am}$ -Be source;** ( $B_E$  – spectral source strength,  $B_E = dB/dE$ ,  $B$  – neutron source strength)

- The dose equivalent rate generated by all neutrons at the point of test, including main neutron beam from  $^{241}\text{Am}$ -Be source and scattered neutrons, was defined as  $E$ .
- The dose equivalent rate caused by only scattered neutrons at the point of test was defined as  $C$ .
- The ratio between  $C$  and  $E$  was the contribution rate of scattered neutrons and it was defined as  $R$ .

### Free field reference neutron radiation

In ISO-8529 series standards, the FRNR is defined for irradiators performed in free space with no scatter or background effects. In our simulation work,  $^{241}\text{Am}$ -Be radionuclide source was placed in the geometric centre of the place large enough and the medium was air. FRNR is the simplest reference neutron radiation. Simulation work on FRNR is applied for comparing with the SRNR and MRNR, which will help us to understand the SRNR and MRNR well.

### Standard reference neutron radiation

In ISO-8529, three type of rooms for SRNR building are regulated. The room type includes cubical type room, half-cubical type room and open ceiling room. Table 1 shows the minimum room length for 40 % room return of  $^{241}\text{Am}$ -Be radionuclide source.  $L$ ,  $W$ , and  $H$  are the length, width and height of the room respectively.

In this study, open ceiling room was not in consideration. The sizes of cubical and half-cubical type room were set as is shown in tab. 1. Thicknesses of each side were set as 0.3 m. In the simulation, different shield materials, borated 5 % polyethylene, concrete, lead and iron, were applied for research. The  $D$  were set as 0.75 m, 0.85 m, 0.95 m, 1.05 m, 1.15 m, 1.25 m, and, 1.35 m, respectively. The schematic of the two reference radiations were shown in fig. 2.

### Minitype reference neutron radiation

Compared to SRNR, there are no relative laws to regulate the size of MRNR and it is a non-standard reference radiation. Considering it is a removable device and should be available, three rules below should be followed when designing a MRNR.

**Table 1. Minimum room length for 40 % room return of  $^{241}\text{Am}$ -Be radionuclide source ( $D = 75\text{ cm}$ )**

Room type	Cubical type room ( $L = W = H$ )	Half-cubical type room ( $L = W = 2H$ )	Open ceiling ( $L = W = 2H$ )
Minimum size	3.0 m	4.3 m	2.9 m

Figure 2. Model of SRNR

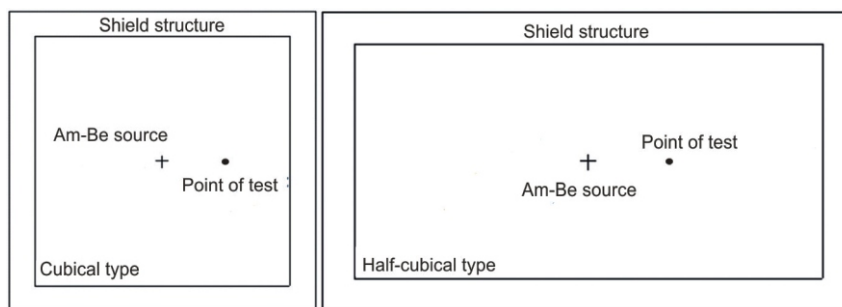


Table 2. The MRNR with different sizes

Length [m]	Width [m]	Height [m]
2.3	1.5	1.5
2.2	1.4	1.4
2.1	1.3	1.3
2	1.2	1.2
1.9	1.1	1.1
1.8	1	1

- The space of MRNR should be able to contain radionuclide neutron source, source container, neutron measuring instrument and its support platform. Moreover, the above quantity *D* should not less than 75 cm. Based on the above conditions, the size and weight should be as small as possible.
- Thickness of the shield box of MRNR should be as thin as possible in the basic of meeting the radiation shield requirements.
- Scattered neutron components in MRNR should be reduced as much as possible in the condition of proper size and shield materials range.

Based on the aforementioned rules, series MRNR with proper sizes, shown in tab. 2, were applied for simulation.

The 5 % borated polyethylene was selected as the shield material and the thickness was set to 0.3 m. Distance between <sup>241</sup>Am-Be radionuclide source and left side of the shield box was kept 0.3 m. The *D* were still set as 0.75 m, 0.85 m, 0.95 m, 1.05 m, 1.15 m, 1.25 m, 1.35 m. The medium in the MRNR was air. The physical model of the MRNR is shown in fig. 3.

### Shadow cone

According to ISO-8529 series standards, shadow cone method is an important correction method of *C* in

the calibration. It can measure the *C* directly. Shadow cone is consisted of two parts: front part made of iron and rear part made of 5 % borated polyethylene. In the simulation work, the cone angle was set as 18°. The lengths of the front part and rear part were 20 cm and 30 cm, respectively. Distance between the <sup>241</sup>Am-Be source and shadow cone was kept at 10 cm for different reference neutron radiations.

## RESULT OF SIMULATION AND DISCUSSION

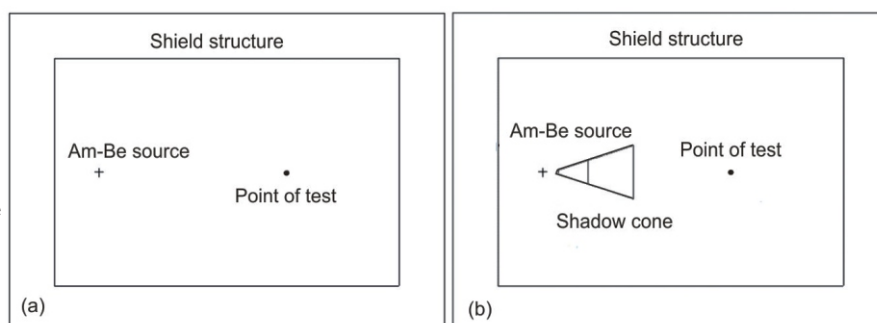
### Characteristics of FRNR

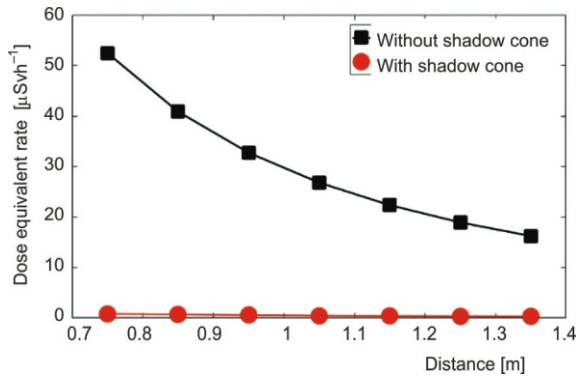
Dose equivalent rate in neutron radiation field is calculated through fluence at the point and fluence-dose equivalent rate conversion coefficient from ICRP 74 report. Fluences at different points were simulated by Monte Carlo method. Distribution of dose equivalent rates in FRNR with and without shadow cone are shown in fig. 4.

From fig. 4, we noticed that distribution of *E* in the FRNR, without shadow cone and distance, followed the inverse-square law. Although, as we have known, that the shadow cone shielded almost all neutrons from <sup>241</sup>Am-Be radionuclide source and the values of *E* reduced sharply at different points of test but, they were still not zeros. The effects we analyzed may be from the air scattered neutrons, which were the *C* mentioned above. The *C* presented decrease trend with the increase of *D*. Table 3 shows the calculated contribution proportions *R* of *C*. The *R* presents the inverse relationship compared to the *E* with the *D* increase.

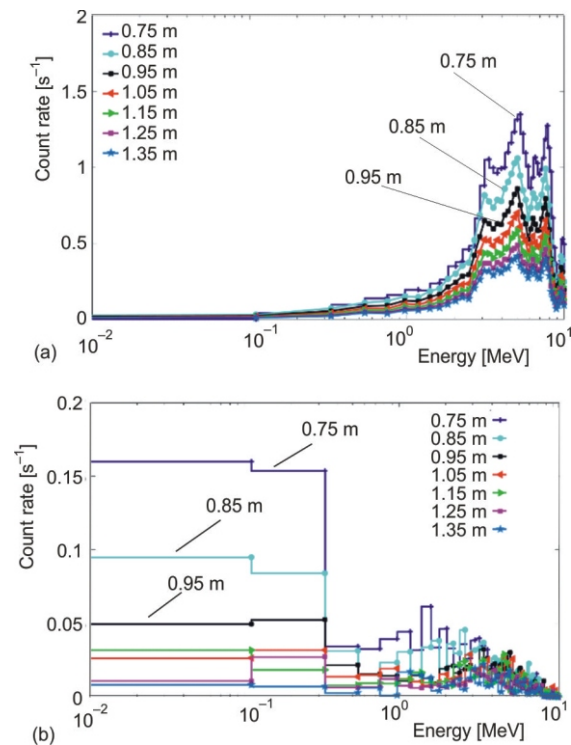
For further research, neutron energy spectra distributions were simulated with and without shadow cone, at different points of test. The results are shown in fig. 5.

Figure 3. Physical model of MRNR; (a) without shadow cone and (b) with shadow cone





**Figure 4. Distribution of dose equivalent rates in FRNR with and without shadow cone**



**Figure 5. Neutron energy spectra at different points of test; (a) without shadow cone and (b) with shadow cone**

In the FRNR, count rates of neutron energy spectra, at different points of test, decrease regularly with the increase of *D*, according to the fig. 5(a). The shapes of the spectra were similar with the pure <sup>241</sup>Am-Be neutron spectrum. In fig. 5(b), due to the shield effect of the shadow cone, the distributions of the spectra were chaotic with low count rates. Count rates of the neutrons with low energy were higher than those with high energy. In general, the FRNR was an ideal reference neutron radiation field. The characteristics of it were easy to be understood.

**Characteristics of standard reference neutron radiation**

In ISO-8529 series, the usual shield material of a SRNR is concrete. Other common shield materials for neutron radiation field are borated polyethylene and paraffin. Considering that in neutron radiation field may exist interactions which may generate gamma rays, lead and iron are usually applied for shielding gamma rays. Therefore, concrete, 5 % borated polyethylene, lead and iron were applied for the shield materials in our simulation work. The dose equivalent rates distributions in SRNR with different shield materials are shown in fig. 6.

From fig. 6, with *D* increasing, dose equivalent rates showed decrease trend at different points of test in SRNR with different shield materials, which were the same with the FRNR. However, no matter whether in cubical type room or in half-cubical type room, the dose equivalent rates, at points of test, were larger than those in FRNR. It was because the neutrons from <sup>241</sup>Am-Be source interacted with the shield wall and a large number of scattered neutrons were generated. The contributions to dose equivalent rates in SRNR compared to FRNR are shown in fig. 7.

According to figs. 6 and 7, SRNR with four shield materials which were sorted as lead, iron, concrete and 5 % borated polyethylene, according to *C* from big to small at the same point of test. Comparing the four materials, the *C* in SRNR constructed of 5 % borated polyethylene or concrete were smaller than in SRNR constructed of lead and iron, obviously. It was because 5 % borated polyethylene and concrete contained a large number of hydrogen atoms, which possess strong moderation and absorption ability to neutrons. For lead and

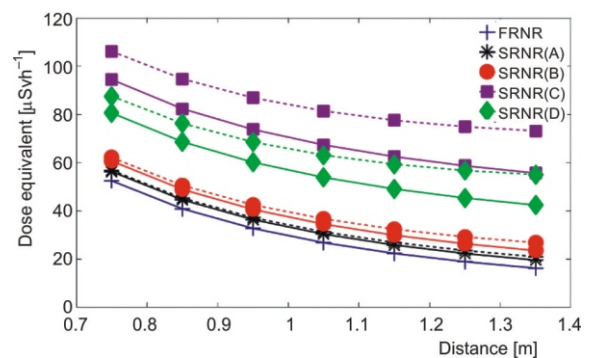


**Figure 6. Distributions of dose equivalent rates in SRNR with different shield materials – (A) 5% Borated polyethylene, (B) Concrete, (C) Lead, (D) Iron; Solid line shows half-cubical type room and Dotted line shows was cubical type room)**

**Table 3. Contribution of scattered neutrons to dose equivalent rate at different points**

Distance [m]	0.75	0.85	0.95	1.05	1.15	1.25	1.35
Contribution of scattered neutrons	1.54 %	1.69 %	1.71 %	1.75 %	1.79 %	1.80 %	1.85 %

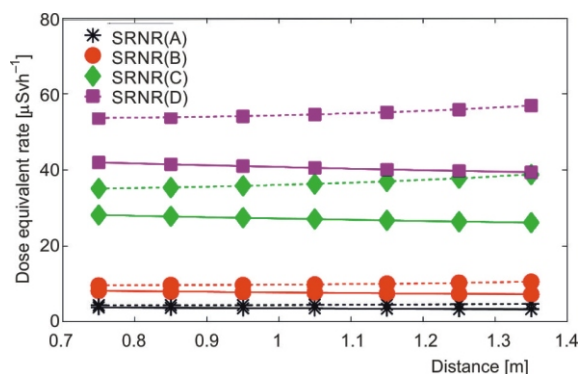


**Figure 7. Contributions to dose equivalent rates in SRNR: shield material: (A) 5 % Borated polyethylene, (B) Concrete, (C) Iron, (D) Lead; Solid line presents half-cubical type room and Dotted line was presents cubical type room**

iron, the absorption and moderation ability are relatively weak. The above results indicated that 5 % borated polyethylene was the most proper shield material for neutron radiation theoretically. However, due to the high cost for building such a large SRNR for actual application, institutes usually choose concrete instead of 5 % borated polyethylene. The *C* in half-cubical type room were smaller than those in cubical type room due to its bigger size, which lead to fewer scattered neutrons. Besides, we noticed an interesting phenomenon that with the increase of *D*, the *C* presented decrease trend in half-cubical type room while increase in cubical type room. It may be easy to understand that the *C* will decrease with the increase of *D*. However, for cubical-room with such a small size, with the increase of *D*, the point of test is close to the inner wall of radiation field, and the scattered neutrons from inner wall of the radiation field were stronger than the attenuation caused by the increase of *D*. The *C* in SRNR varies a little at different locations, but the dose equivalent rates caused by main neutron beam and scattered neutrons, were decreasing with the increase of *D*. Therefore, *C* increases with the increase of *D*. According to *C* and *E* in SRNR, *R* can be calculated, which is shown in tab. 4.

From tab. 4, the *R* in SRNR with different shield materials were all increasing with the increase of *D*. When the shield materials were 5 % borated polyethylene or concrete, the *R* were less than 40 % at all of the points of test. When the shield material was concrete,

the values of *R* were about twice of that shielded by 5 % borated polyethylene.

The *C* at different points of previous test, were achieved according to FRNR and they were treated as ideal *C*. In actual work, shadow cone is widely used for achieving the actual *C*. In order to compare the difference between the ideal *C* and actual *C*, we carried out the simulation on the SRNR with shadow cone. The ideal *C* and actual *C* are presented in tab. 5, as well as the errors between them.

From tab. 5, the errors between ideal *C* and the actual *C* increase with the increase of *D* overall in cubical type room. In half-cubical type room, when 5 % borated polyethylene was employed as the shield material, the errors present a decrease trend with the increase of *D*. When the shield material was concrete, the errors were all within 4 %. The above results indicated that there was obvious difference between the ideal *C* and actual *C*, especially in cubical type room with such size, which will help us to identify the situations of shadow cone.

In order to study the neutron composition at different points of test, the neutron energy spectra were simulated. The neutron energy spectra distributions of cubic type room and half-cubical type room, at different points of test, are shown in figs. 8 and 9, respectively. Lead and iron materials were not in consideration. The left figure is the whole neutron energy spectrum and the right figure presents the range of count rate from 0 s<sup>-1</sup> to 2 s<sup>-1</sup>. Similar figures below were all applied for this presentation style.

When the shield material was concrete or borated polyethylene, the counts of each energy channel of the neutron energy spectra, at different locations, decrease regularly with the increase of *D*. The shape of energy spectrum above 2 MeV is similar to that of <sup>241</sup>Am-Be neutron source. The energy spectrum of the energy band within 2 MeV is different from that of the <sup>241</sup>Am-Be neutron source due to the increase of counts. Compared to concrete, the count rate increased less below 2 MeV in SRNR shielded by 5 % borated polyethylene.

### Characteristics of MRNR

Compared with SRNR, the design idea of MRNR was lightweight. It means that the size and vol-

**Table 4. The *R* in SRNR with different shield materials**

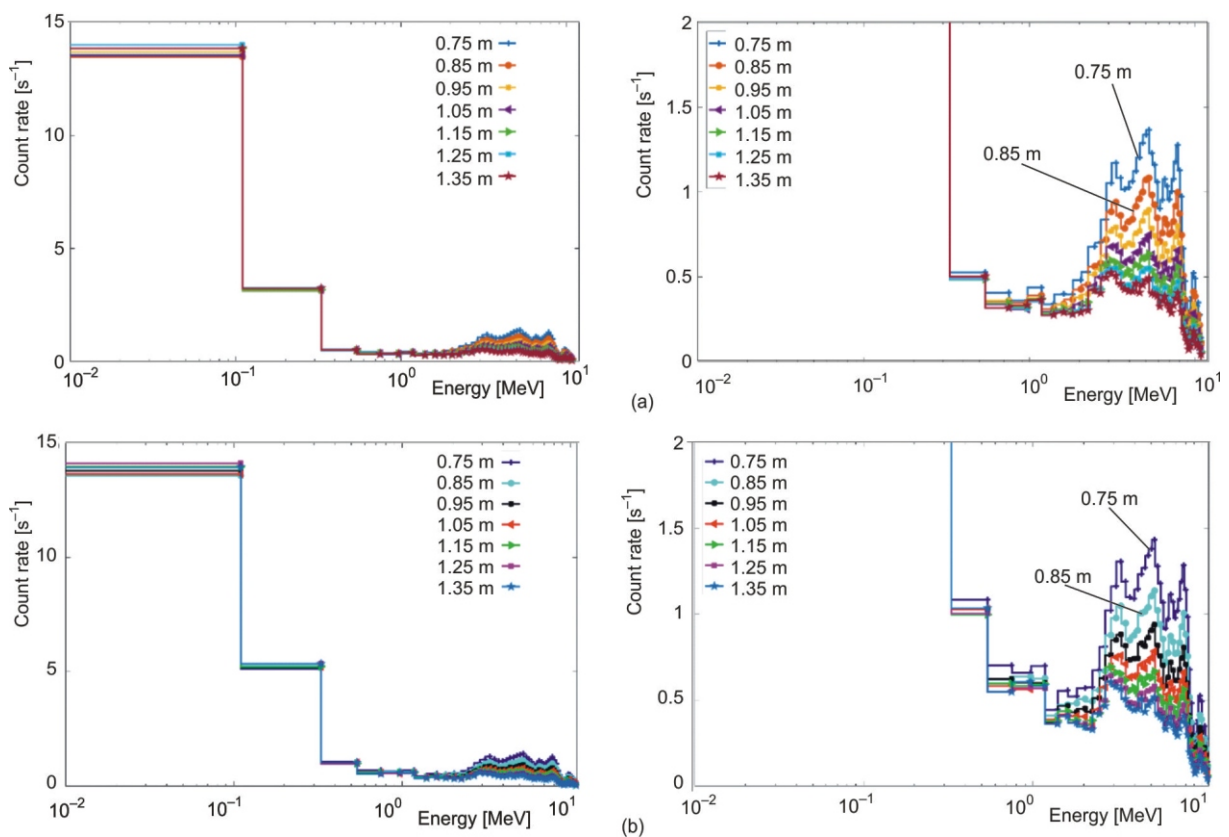
Room type	0.75 m	0.85 m	0.95 m	1.05 m	1.15 m	1.25 m	1.35 m
Cubical (A*)	7.70 %	9.72 %	11.94 %	14.34 %	16.91 %	19.66 %	22.60 %
Half-cubical (A)	6.79 %	8.37 %	10.02 %	11.71 %	13.45 %	15.22 %	17.01 %
Cubical (B)	15.54 %	19.18 %	22.98 %	26.92 %	30.98 %	35.17 %	39.50 %
Half-cubical (B)	13.51 %	16.39 %	19.33 %	22.29 %	25.23 %	28.14 %	31.00 %
Cubical (C)	40.08 %	46.41 %	52.24 %	57.53 %	62.32 %	66.62 %	70.50 %
Half-cubical (C)	34.90 %	40.46 %	45.56 %	50.23 %	54.44 %	58.25 %	61.70 %
Cubical (D)	50.57 %	56.85 %	62.33 %	67.07 %	71.17 %	74.71 %	77.80 %
Half-cubical (D)	44.45 %	50.37 %	55.61 %	60.20 %	64.22 %	67.73 %	70.82 %

\* Shield materials: (A) 5 % borated polyethylene, (B) Concrete, (C) Iron, and (D) Lead

**Table 5. Comparison of the ideal  $C$  and actual  $C$  in different room type reference neutron radiation with different shield materials (unit:  $\text{Sv h}^{-1}$ )**

Room type		0.75 m	0.85 m	0.95 m	1.05 m	1.15 m	1.25 m	1.35 m
Cubical (A) *	Ideal $C$	4.38	4.40	4.44	4.49	4.55	4.63	4.74
	Actual $C$	4.54	4.54	4.40	4.25	4.06	3.80	3.47
	Error	3.74 %	3.11 %	-0.81 %	-5.35 %	-10.84 %	-17.86 %	-26.90 %
Half-cubical (A)	Ideal $C$	3.82	3.73	3.64	3.55	3.47	3.40	3.33
	Actual $C$	4.33	4.25	4.07	3.89	3.72	3.57	3.43
	Error	13.38 %	13.83 %	11.70 %	9.46 %	7.20 %	5.09 %	3.06 %
Cubical (B)	Ideal $C$	9.65	9.69	9.77	9.87	10.04	10.27	10.60
	Actual $C$	9.08	9.21	9.11	8.92	8.66	8.28	7.71
	Error	-5.95 %	-4.91 %	-6.73 %	-9.59 %	-13.75 %	-19.38 %	-27.31 %
Half-cubical (B)	Ideal $C$	8.19	8.01	7.84	7.69	7.54	7.41	7.30
	Actual $C$	8.20	8.30	8.09	7.84	7.61	7.39	7.17
	Error	0.11 %	3.62 %	3.16 %	1.98 %	0.93 %	-0.32 %	-1.73 %

\* Shield materials: (A) 5 % borated polyethylene and (B) concrete

**Figure 8. Neutron energy spectra distribution in cubical type room: shield materials; (a) 5 % borated polyethylene and (b) concrete**

ume should be as small as possible. Meanwhile, it should be able to contain the neutron radionuclide source, source container and the detector to be calibrated. In the second section of this paper, the size of MRNR series that meets the requirements, is listed. After comparing the four shield materials, 5 % borated polyethylene was the best shield material for constructing an MRNR with such small size. The distributions of  $E$  and  $C$  are shown in fig. 10 respectively.

From fig. 10, the  $E$  in MRNR increase more than those in SRNR. With the increase of distance between

$^{241}\text{Am-Be}$  source and point of test, the  $C$  showed decrease trend, which was obviously different from SRNR shown in fig. 7. According our analysis, the  $^{241}\text{Am-Be}$  source was not located at the geometric center but near the side of MRNR. Therefore, the closer to the radiation source, the more scattered neutron components from the wall scattered, which lead a larger contribution to dose equivalent rate. Table 6 showed the  $R$  in MRNR with different sizes.

It indicated that when the shield material was 5 % borated polyethylene, the MRNR with the size of

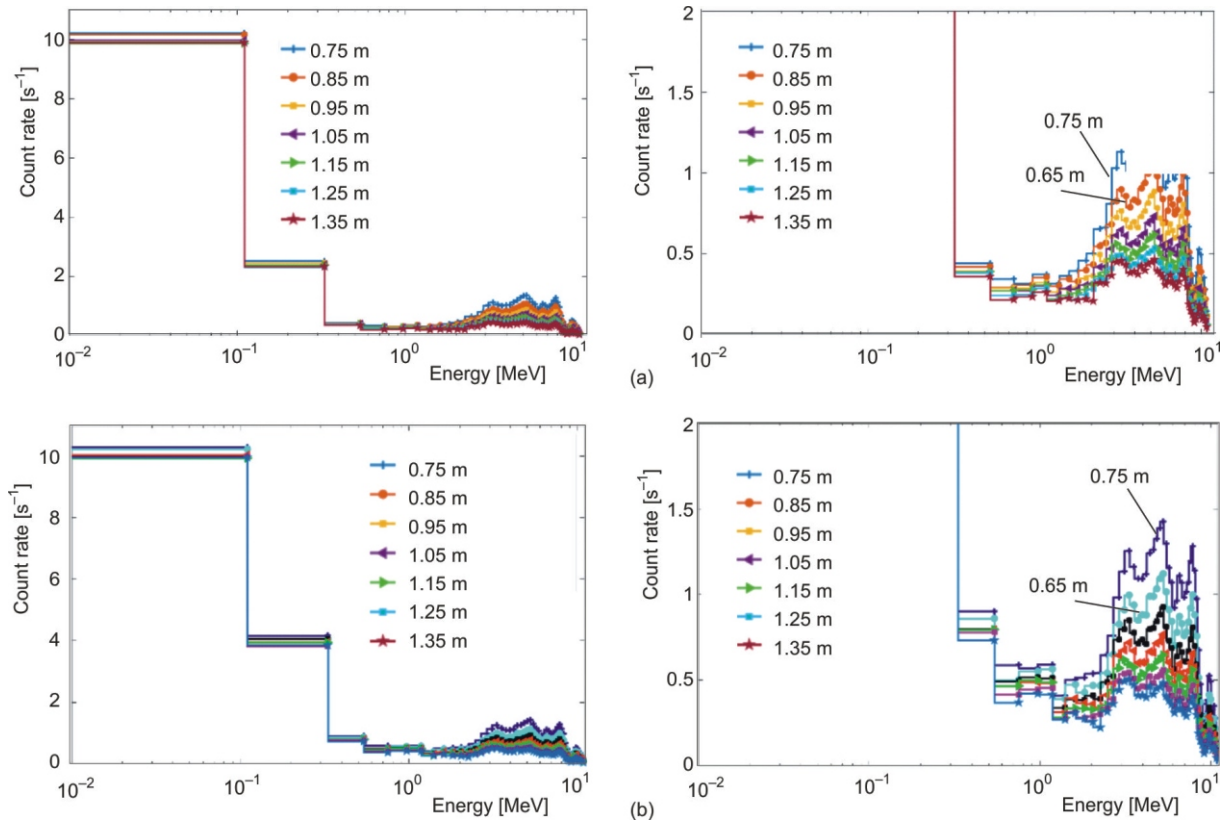


**Figure 9. Neutron energy spectra distribution in half-cubical type room: shield materials; (a) 5 % borated polyethylene and (b) concrete**

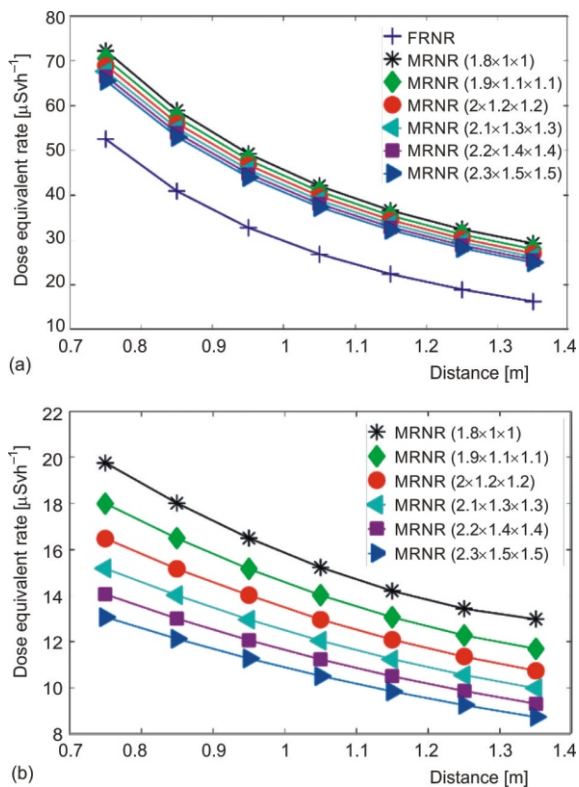


**Figure 10. Distributions of  $E$  and  $C$  in MRNR: (a)  $E$  and (b)  $C$**

$2\text{ m} \times 1.2\text{ m} \times 1.2\text{ m}$  was a proper design because the contribution proportions were all less than 40 % at points of test in the range of 0.75 m-1.35 m. Based on this, the ideal  $C$  and actual  $C$  were simulated to understand if shadow cone was proper to be applied in MRNR with the size of  $2\text{ m} \times 1.2\text{ m} \times 1.2\text{ m}$ . The results were shown in tab. 7.

From tab.7 we noticed that the errors between ideal  $C$  and actual  $C$  were stable except that for  $D$  equal to 0.75 m and 0.85 m. Compared to SRNR, the errors showed different trends with the increase of  $D$ . Therefore, when shadow cone is employed in SRNR or MRNR, more attention should be paid to the points of test which were close to the inner wall of radiation or to the  $^{241}\text{Am-Be}$  source.

In addition to the dose equivalent rate distribution of MRNR, we also simulated the energy spectrum distribution of MRNR. For the MRNR of  $2\text{ m} \times 1.2\text{ m} \times 1.2\text{ m}$ , the distribution of energy spectrum, at different points of test, is shown in fig. 11.

Compared with the energy spectrum distribution of SRNR and FRNR, the increase of neutron count rate in MRNR is significant in the energy range below 2 MeV. The maximum value of the neutron spectrum had risen dozens of times. From the distribution of the spectra, there were a large number of scattered neutrons in the MRNR, which changed the spectrum components. Therefore, for neutron measurement instruments with

**Table 6. The *R* in MRNR with different sizes**

Size [m]	0.75 m	0.85 m	0.95 m	1.05 m	1.15 m	1.25 m	1.35 m
2.3 × 1.5 × 1.5	19.94 %	22.86 %	25.59 %	28.15 %	30.53 %	32.78 %	34.91 %
2.2 × 1.4 × 1.4	21.13 %	24.12 %	26.92 %	29.51 %	31.92 %	34.21 %	36.39 %
2.1 × 1.3 × 1.3	22.44 %	25.53 %	28.36 %	30.98 %	33.44 %	35.77 %	38.02 %
2.0 × 1.2 × 1.2	23.91 %	27.05 %	29.98 %	32.58 %	35.07 %	37.46 %	39.79 %
1.9 × 1.1 × 1.1	25.55 %	28.74 %	31.65 %	34.33 %	36.86 %	39.32 %	41.84 %
1.8 × 1.0 × 1.0	27.37 %	30.59 %	33.51 %	36.22 %	38.83 %	41.49 %	44.39 %

\* Shield materials: 5 % borated polyethylene

**Table 7. Comparison of the ideal *C* and actual *C* in MRNR (2.0 m × 1.2 m × 1.2 m) (unit: Sv<sup>-1</sup>)**

	0.75 m	0.85 m	0.95 m	1.05 m	1.15 m	1.25 m	1.35 m
Ideal <i>C</i>	16.48	15.15	14.01	12.95	12.08	11.34	10.73
Actual <i>C</i>	12.97	13.33	12.76	11.84	11.14	10.41	9.75
Error	-21.26 %	-12.01 %	-8.97 %	-8.57 %	-7.71 %	-8.20 %	-9.12 %

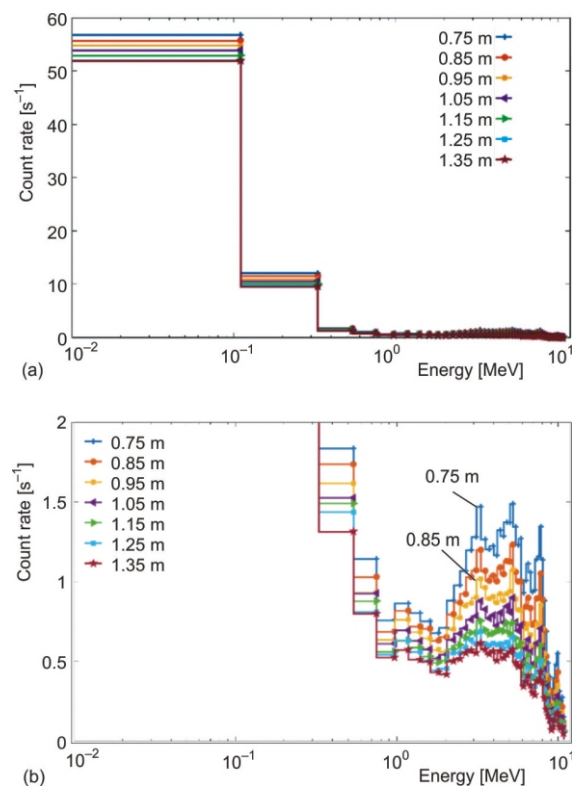


**Figure 11. Neutron energy spectra distribution in MRNR with size of 2 m × 1.2 m × 1.2 m; (a) the whole neutron energy spectrum and (b) range of count rate from 0 s<sup>-1</sup> to 2 s<sup>-1</sup>**

different energy response, a great difference may exist in the measuring results.

**Comparison of the three types of reference neutron radiation**

Based on the previous simulation, comparison of the three types of reference neutron radiation was proposed. In the comparison, the shield material of the SRNR and MRNR was 5 % borated polyethylene. The

size of MRNR was selected as 2 m × 1.2 m × 1.2 m, according to our estimation. The comparison included distribution of dose equivalent rates and neutron energy spectra.

First, the distribution of equivalent rate, *E* and scattered contribution, *R* for three types of reference neutron radiation, were shown in fig. 12.

From fig. 12, the increases of dose equivalent rate in MRNR were more obvious than that in SRNR. The scattered contributions from scattered neutrons in MRNR were about three times bigger than in SRNR. All *R* calculated by actual *C* were smaller than that for ideal *C*. This phenomenon is more obvious in MRNR. It means that the shadow cone is more proper to be em-

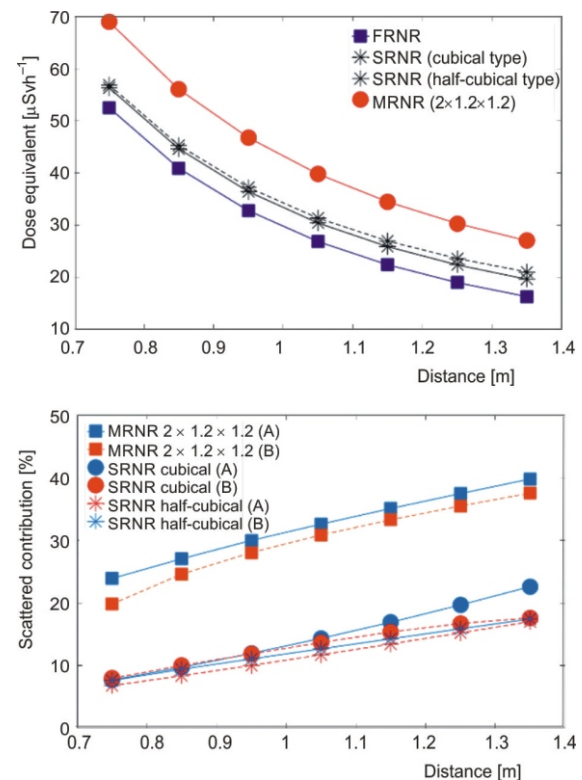


**Figure 12. The *E* and *R* of three type of reference neutron radiation; (A) ideal *C* and B, actual *C***

ployed in SRNR with large size, which is accordant with the standards.

In the comparison of the distribution of neutron energy spectra, the point of test was at the distance of 0.75 m to the  $^{241}\text{Am}$ -Be source. Comparison is shown in fig. 13.

From fig. 13, the neutron energy spectrum in FRNR was similar to the pure  $^{241}\text{Am}$ -Be neutron energy spectrum. For SRNR and MRNR, the count rate in the energy range above 5 MeV was almost the same as that for FRNR. However, in the energy range below 5 MeV, with the decrease of energy, the count rate increased gradually.

### Discussion on the feasibility of MRNR for calibration

From the previous simulation results, it can be seen that the dose equivalent rate distribution and energy spectrum distribution, of the three types of neutron reference radiation fields, are quite different. Although, the contribution from scattered neutrons in the MRNR with the size of  $2\text{ m} \times 1.2\text{ m} \times 1.2\text{ m}$ , or larger, was less than 40 %, at the points of test within 0.75 m-1.35 m range, it was still significant and should be corrected. The shadow cone technology was proved to be employed in reference neutron radiations with large size above. In addition to the shadow cone method mentioned above, there are still another three scattered

neutron correction methods: the generalized fit method, the semi-empirical method and the reduced fitting method. The latter three methods, when the radiation field, detectors and other required conditions are fulfilled, the correction results of the different methods agree reasonably well. Besides, there are strong limitations on the type and geometry of the instruments to be calibrated and the  $^{241}\text{Am}$ -Be source should be located at the geometric center of the radiation field. Therefore, the above scattered neutron correction methods are not proper for the calibration in MRNR. If we want to apply MRNR for the calibration of neutron measurement instruments, reasonable and effective neutron scattering correction method should be developed.

Besides, from to the energy response view, the distribution of neutron energy spectra at the points of test in MRNR showed a significant variation in the  $^{241}\text{Am}$ -Be spectrum (specially in the epithermal region). The energy response of different neutron measurement instruments may vary greatly. This difference will lead to great errors in the measurement results. Therefore, the application limitation of MRNR should be taken into consideration. In the future, a lot of research should be done on the energy response correction method of MRNR for neutron measurement instrument calibration.

### CONCLUSIONS

According to our simulation research, for reference neutron radiation generated by  $^{241}\text{Am}$ -Be radionuclide source, the FRNR was the ideal reference radiation. The structure of FRNR is simple and the dose equivalent rates at each points of test in the field and the distance to the  $^{241}\text{Am}$ -Be source, follow the inverse square attenuation relationship. Contributions to the dose equivalent rate from scattered neutrons were small and they can be neglectable. However, it is impossible to build such a reference radiation.

The sizes of the SRNR in our simulation work were set as the minimum value regulated by ISO-8529 series standards. Contributions to the dose equivalent rates in SRNR from scattered neutrons were obvious. When 5 % borated polyethylene or concrete were used as the shield materials, contributions from scattered neutrons decreased obviously due to the strong moderation and absorption ability for neutrons. Based on the above simulation work, points of test in the range of 0.75 m-1.35 m from the  $^{241}\text{Am}$ -Be all meet the requirement that the contribution of scattered neutrons is less than 40 %. In practice, the SRNR can be enlarged to make its characteristics closer to the FRNR.

For MRNR, the size of  $2\text{ m} \times 1.2\text{ m} \times 1.2\text{ m}$  was a proper design when it was shielded by 5 % borated polyethylene. However, there is still a large number of scattered neutrons, which changes the distribution of

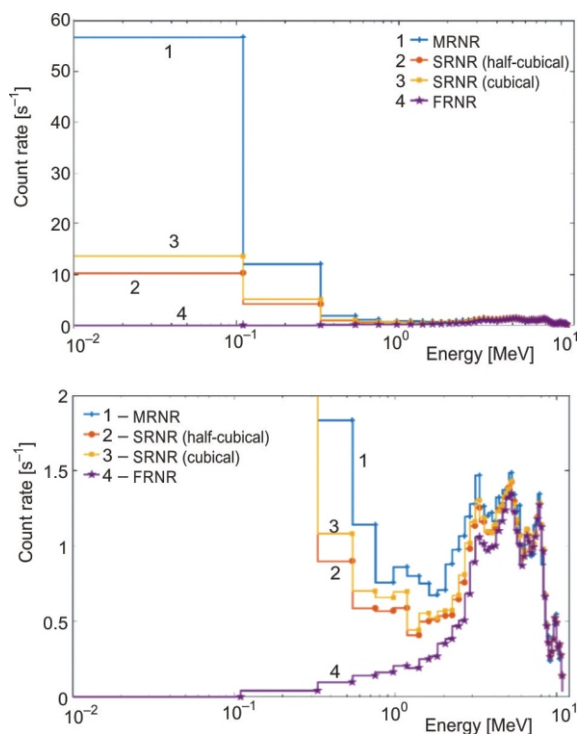


Figure 13. Comparison of the neutron spectra distribution in the three types of reference neutron radiation

the neutron spectrum compared to FRNR. The dose equivalent rate increases obviously. The actual *C*, calculated through the shadow cone technology, shows obvious deviation compared to the ideal *C*. Therefore, if the MRNR is applied for the calibration of neutron measurement instruments, proper scattering correction method should be developed. Moreover, study on the deviation caused by different energy response of neutron measurement instruments and energy response correction methods, should be carried out in the future work.

#### DATA AVAILABILITY

The data used to support the findings of this study are available from the corresponding author upon request.

#### ACKNOWLEDGMENT

This work was supported by National Natural Science Foundation of China (grant number: 11805111); The Fundamental Research Funds for the Central Universities (grant number: 2018CDGFGD0008).

#### AUTHOR'S CONTRIBUTIONS

The simulated data were organized and analyzed by Y. Liu. The manuscript was also written by Y. Liu. Z. Chen is the manuscript corresponding author and provided the research ideas and methods. S. Zhang has executed the development of the Monte Carlo code. Y. Qian, Y. Huang, B. Mao, and P. Feng discussed the results and put forward many insightful opinions about modeling, coding and theoretical analyzing.

#### REFERENCES

- [1] Thomas, D. J., *et al.*, Neutron Metrology FOREWORD, *Metrologia*, 48 (2011), 6
- [2] Thomas, D. J., *et al.*, What is Neutron Metrology and Why is it Needed?, *Metrologia*, 48 (2011), 6, pp. S225-S238
- [3] Gressier, V., *et al.*, Calibration of Neutron-Sensitive Devices, *Metrologia*, 48 (2011), 6, pp. S313-S327
- [4] Roberts, N. J., *et al.*, Radionuclide Neutron Source Characterization Techniques, *Metrologia*, 48 (2011), 6, pp. S239-S253
- [5] \*\*\*, ISO 8529-1:2001, Reference Neutron Radiations – Part 1 : Characteristics and Methods of Production, 2001-02, <https://www.iso.org/standard/25666.html>
- [6] \*\*\*, ISO 8529-2:2000, Reference Neutron Radiations – Part 2: Calibration Fundamentals of Radiation Protection Devices Related to the Basic Quantities Characterizing the Radiation Field, 2000-08, <https://www.iso.org/standard/25667.html>
- [7] \*\*\*, ISO 8529-3:1998, Reference Neutron Radiations – Part 3: Calibration of Area and Personal Dosimeters and Determination of Their Response as a Function of Energy and Angle of Incidence, 1998-11, <https://www.iso.org/standard/25668.html>
- [8] \*\*\*, ISO 12789-1:2008, Reference Radiation Fields – Simulated Workplace Neutron Fields – Part 1: Characteristics and Methods of Production, 2008-03, <https://www.iso.org/standard/46369.html>
- [9] \*\*\*, ISO 12789-2:2008, Reference Radiation Fields – Simulated Workplace Neutron Fields – Part 2: Calibration fundamentals Related to the Basic Quantities, 2008-03, <https://www.iso.org/standard/37366.html>
- [10] Lacoste, V., *et al.*, Simulated Workplace Neutron Fields, *Metrologia*, 48 (2011), 6, pp. S304-S312
- [11] Kim, Y. H., *et al.*, Reference Thermal Neutron Field at KRISS for Calibration of Neutron Detectors, *Radiation Measurements*, 107 (2017), pp. 73-79
- [12] Le, T. N., *et al.*, Neutron Calibration Field of a Bare <sup>252</sup>Cf Source in Vietnam, *Nuclear Engineering and Technology*, 49 (2017), 1, pp. 277-284
- [13] Gressier, V., *et al.*, Characterization of a Measurement Reference Standard and Neutron Fluence Determination Method in IRSN Monoenergetic Neutron Fields, *Metrologia*, 51 (2014), 5, pp. 431-440
- [14] Liu, Y., *et al.*, Determination of the Conventional True Value of Gamma-Ray Air Kerma in a Minitype Reference Radiation, *Applied Radiation and Isotopes*, 118 (2016), pp. 238-245
- [15] Liu, Y. X., *et al.*, Feasibility Study on Determining the Conventional True Value of Gamma-Ray Air Kerma in a Minitype Reference Radiation, *Nuclear Science and Techniques*, 28 (2017), 6, pp. 80 (1-7)
- [16] Bayrak, A., *et al.*, A Segmented Neutron Detector Based on Silicon-PIN Photodiodes Using Neutron-Proton Converters, *Nucl Technol Radiat*, 34 (2019), 2, pp. 138-144
- [17] Sokolov, A., *et al.*, The Development of Waste Assay Monitors Based on the HPGe Detectors, *Nucl Technol Radiat*, 33 (2018), 4, pp. 411-416
- [18] Agostinelli, S., *et al.*, Geant4-a Simulation Toolkit, Nuclear Instruments and Methods in Physics Research Section A: Accelerators, Spectrometers, Detectors and Associated Equipment, 506 (2003), 3, pp. 250-303

Received on October 4, 2019

Accepted on November 29, 2020

**Јисин ЉУ, Сунг ЦАНГ, Јикуен ЂЕН, Јучен ХУАНГ, Бенгђанг МАО, Пенг ФЕНГ, Циђанг ЧЕН**

**ПРОУЧАВАЊЕ МОНТЕ КАРЛО СИМУЛАЦИЈОМ РЕФЕРЕНТНОГ  
НЕУТРОНСКОГ ЗРАЧЕЊА ИЗ  $^{241}\text{Am-Be}$  ИЗВОРА РАДИОНУКЛИДА**

Да би се проучила употребљивост поља референтног неутронског зрачења од лаког  $^{241}\text{Am-Be}$  извора за калибрацију инструмената за мерење неутрона, у овом раду је изложена Монте Карло симулација слободног поља референтног неутронског зрачења регулисаног ИСО-серијом стандарда и референтног неутронског зрачења минитипа, које смо дизајнирали. Расподела јачина еквивалентне дозе и неутронског енергетског спектра у различитим условима, као што су различити типови и величине просторија и различити заштитни материјали, били су главни предмети симулације за анализу карактеристика три врсте референтног неутронског зрачења. Према резултатима симулације, добијене су теоријске основе за расправу о минитип референтном неутронском зрачењу у сврху калибрације.

*Кључне речи: Монте Карло,  $^{241}\text{Am-Be}$  извор радионуклида, референсно неутронско зрачење, неутронски енергетски спектар, јачина еквивалентне дозе*

---